# Differential neural correlates of reciprocal activation and cocontraction control in dorsal and ventral premotor cortices

**Masahiko Haruno, Gowrishankar Ganesh, Etienne Burdet and Mitsuo Kawato**

*J Neurophysiol* 107:126-133, 2012. First published 12 October 2011; doi:10.1152/jn.00735.2010

*J Neurophysiol* 107: 126–133, 2012.
First published October 12, 2011; doi:10.1152/jn.00735.2010.

# Differential neural correlates of reciprocal activation and cocontraction control in dorsal and ventral premotor cortices

**Masahiko Haruno,[1,2,3,4] Gowrishankar Ganesh,[1] Etienne Burdet,[5] and Mitsuo Kawato[1]**

[1]*ATR Computational Neuroscience Laboratory, Kyoto;* [2]*Center for Information and Neural Networks, National Institute of Information and Communications Technology, Kobe Hyogo;* [3]*PRESTO, Japan Science and Technology Agency;* [4]*Tamagawa University Brain Science Institute, Tokyo, Japan; and* [5]*Department of Bioengineering, Imperial College of Science, Technology and Medicine, South Kensington Campus, London, United Kingdom*

Submitted 24 August 2010; accepted in final form 12 October 2011

**Haruno M, Ganesh G, Burdet E, Kawato M.** Differential neural correlates of reciprocal activation and cocontraction control in dorsal and ventral premotor cortices. *J Neurophysiol* 107: 126–133, 2012. First published October 12, 2011; doi:10.1152/jn.00735.2010.—Efficient control of reciprocal activation and cocontraction of the muscles are critical to perform skillful actions with suitable force and impedance. However, it remains unclear how the brain controls force and impedance while recruiting the same set of muscles as actuators. Does control take place at the single muscle level leading to force and impedance, or are there higher-order centers dedicated to controlling force and impedance? We addressed this question using functional MRI during voluntary isometric wrist contractions with online electromyogram feedback. Comparison of the brain activity between the conditions requiring control of either wrist torque or cocontraction demonstrates that blood oxygen level-dependent activity in the caudo-dorsal premotor cortex (PMd) correlates well with torque, whereas the activity in the ventral premotor cortex (PMv) correlates well with the level of cocontraction. This suggests distinct roles of the PMd and PMv in the voluntary control of reciprocal activation and cocontraction of muscles, respectively.

EMG; fMRI; stiffness; torque; motor control

THE NEURAL SUBSTRATES FOR the control of endpoint force or joint torque have been investigated extensively in previous studies. In particular, electrophysiological studies in monkeys showed that during wrist movements, activity of the majority of the primary motor cortex (M1) neurons was correlated with the exerted torque rather than hand displacement (Cheney and Fetz 1980; Evarts 1968; Fetz and Cheney 1980; Jackson et al. 2003). Similarly, functional imaging studies in humans have shown neural correlates of force control in the M1 and other brain structures, including the dorsal and ventral premotor cortices (PMd and PMv, respectively), the supplementary motor area (SMA), the cerebellum, and basal ganglia (Dai et al. 2001; Dettmers et al. 1995; Pope et al. 2005; Vaillancourt et al. 2003).

However, skillful control of motor tasks requires more than force production. In particular, tasks involving tools require controlling impedance at the endpoint of the arm, such as maintaining stability when using a screwdriver or producing a stable hit with a tennis racket (Burdet et al. 2001; Damm and McIntyre 2008; Lacquaniti and Maioli 1989; Perreault et al. 2001). A major property of the human musculoskeletal system is that its impedance can be tuned by the central nervous system (CNS). Impedance covaries with activation in a single muscle, but endpoint impedance can be controlled independently from force by coordinating the activation of multiple muscles (Burdet et al. 2001). Roughly speaking, at a joint, torque is exerted by reciprocal activation of the muscles spanning this joint, whereas impedance can be regulated by cocontracting the antagonist muscles.

Therefore, reciprocal and cocontraction control of muscles is central to such motor control theories as the equilibrium-point hypothesis (Bizzi et al. 1984; Feldman 1966; Levin et al. 1992; Ostry and Feldman 2003) and the internal model theory of simultaneous force and impedance control (Franklin et al. 2008). The importance of cocontraction control is also illustrated by dystonia patients who can perform voluntary movements with normal, rapid, reciprocal activation but exhibit excessive cocontraction and sluggish movements when muscle cocontraction is required (Berardelli et al. 1998). This prevents these patients from performing activities of daily living successfully and suggests the possibility of specific neural mechanisms dedicated to controlling reciprocal activation and cocontraction.

To understand the control of force and impedance in humans, we investigated the neural correlates of reciprocal activation (torque) and cocontraction of muscles using functional MRI (fMRI). We used an isometric wrist task so as to reliably measure the activity from contributing muscles (Hoffman and Strick 1999) while avoiding movement artifacts. A fMRI-compatible interface, equipped with a torque sensor (Gassert et al. 2006), as well as an algorithm for online filtering of MRI artifacts on the electromyogram (EMG) signals (Ganesh et al. 2007) were used to achieve a quantitative comparison of brain activity between reciprocal activation and cocontraction.

## METHODS

*Subjects and setup.* Two females and 10 males, all right-handed, healthy adults between 23 and 40 years old, participated in the study. The Institutional Ethics Committee of ATR Computational Neuroscience Laboratory (Kyoto, Japan) approved the experiments, and subjects gave informed consent prior to participation. A fMRI-compatible robotic interface (Gassert et al. 2006) was used to restrain the subject's wrist to an isometric posture with straps and a plastic splint (Fig. 1*A*) while the subject contracted his or her muscles. This device has a custom-made torque sensor that was used to collect wrist joint torque during the experiment. All of the subjects used their right hand to conduct the task.

Address for reprint requests and other correspondence: M. Haruno, Center for Information and Neural Networks, National Institute of Information and Communications Technology, 588-2 Iwaoka-cho Nishiku, Kobe Hyogo 651-2492, Japan (e-mail: mharuno@nict.go.jp).

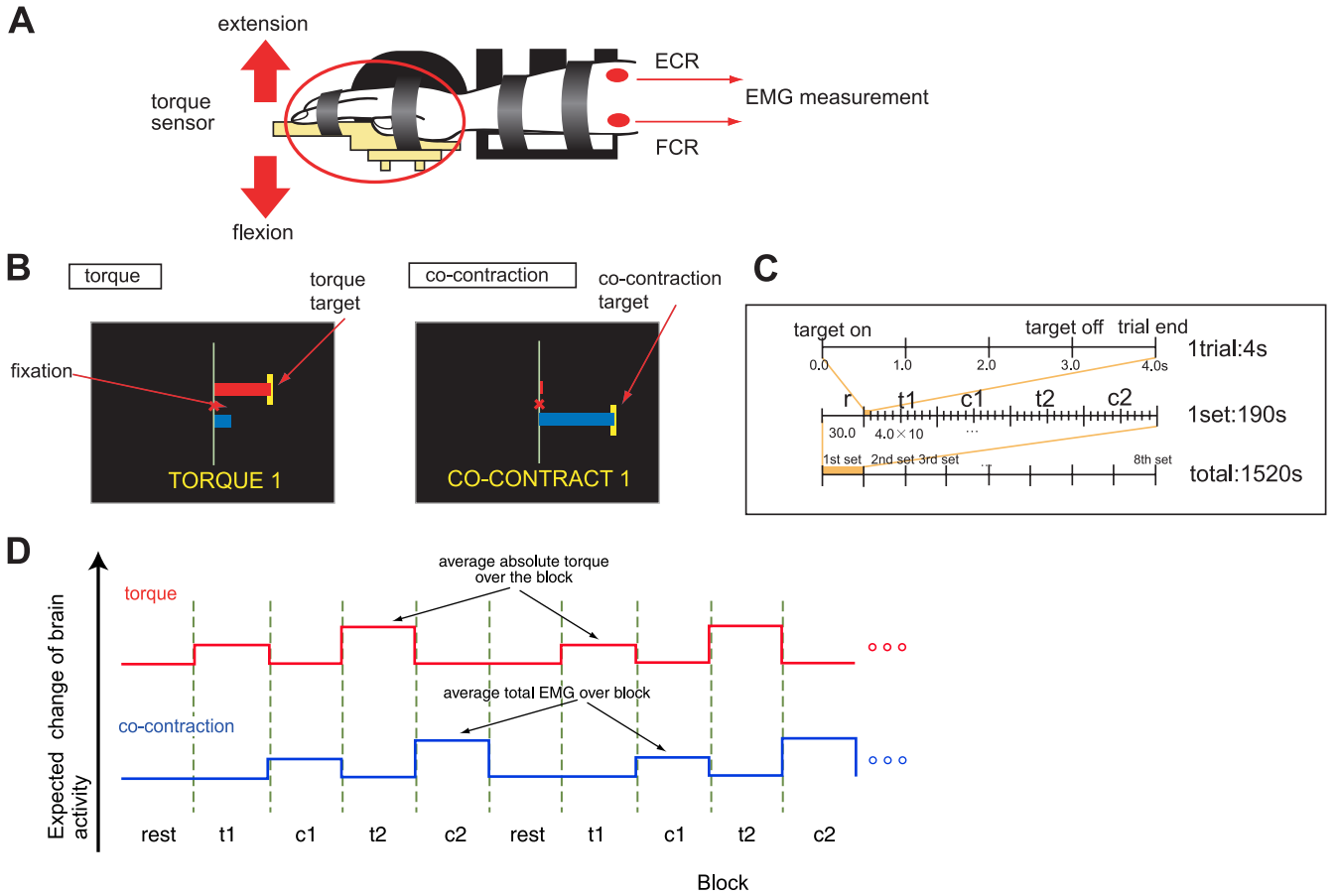


Fig. 1. Task design and timeline. *A*: subjects put their right hand in a wrist flexion/extension MRI-compatible manipulandum with their wrist in the midway position and fingers spread out. Surface electromyogram (EMG) was recorded from extensor carpi radialis brevis + extensor carpi radialis longus (ECR) and flexor carpi radialis (FCR), because they are the dominant muscles actuating wrist flexion-extension. *B*: in the isometric torque condition, subjects increased their wrist torque (red bar) to match a visual target, shown randomly to the left (i.e., flexion) or right (i.e., extension) of the fixation. In the cocontraction condition, subjects held the cocontraction level (blue bar) of the wrist muscles at a target corresponding to average rectified EMG from the previous torque block, displayed randomly to the left or right of the fixation point. *C*: timeline of the task. Each of the 4 task blocks [torques 1 and 2 (t1 and t2) and cocontractions 1 and 2 (c1 and c2)] contained 10 trials and a rest period (r) of 30 s. These 5 blocks were repeated 8 times. One trial in each block lasted for 4 s, and therefore, the total experiment time was 1,520 s [(4 × 10 × 4 + 30) × 8]. *D*: hypothetical brain activity involved in torque and cocontraction conditions. Assuming brain activity is linearly related to amplitude of reciprocal activation, it is expected to increase only in torque conditions with the exerted torque (red line). Similarly, brain activity related to cocontraction will increase with the amplitude of cocontraction, represented as average total EMG of ECR and FCR (blue line) in the cocontraction condition.

*EMG.* During fMRI experiments, EMG was recorded from two muscles acting at the wrist [flexor carpi radialis (FCR) and extensor carpi radialis brevis (ECRB) + extensor carpi radialis longus (ECRL; ECR)]. As selective surface EMG recording from ECRB and ECRL is difficult, ECRB + ECRL will be described as ECR hereafter. FCR and ECR are two major contributors to wrist flexion and extension in the midway position (Haruno and Wolpert 2005; Hoffman and Strick 1999; Kakei et al. 1999).

After electrode placements for each muscle were determined using functional movements, the area was cleansed with alcohol and abrasive gel (Nuprep, Weaver and Company, Aurora, CA). EMG electrodes designed for MRI environments (NE-706A, Nihon Kohden, Tokyo, Japan) were filled with EMG electrode paste (Biotech, GE Marquette Medical Systems, Japan) and firmly taped to the subject's skin. Two electrodes were positioned on the belly of each muscle, separated by ~1 cm. An elastic cloth sleeve was placed over the electrodes and wires, fixing them against the subject's forearm to avoid any accidental electrode removal and to minimize the movements of the electrode wires during scanning. Once the subject was positioned in the scanner, the long, braided electrode wires were firmly fixed to prevent movement in the magnetic field of the scanner. To avoid external noise being carried into the shielded MRI room, the electrode wires were passed through multiple ferrite filters before passing through waveguides in the penetration panel of the MRI room. EMG signals were cleaned online during scanning and used to provide EMG feedback. The details of EMG processing are described in Ganesh et al. (2007).

In a separate session performed outside of the MRI scanner, the EMG signals from four wrist muscles—FCR, ECR, flexor carpi ulnaris (FCU), and extensor carpi ulnaris (ECU)—and four upper-arm muscles—biceps brachii, triceps brachii lateral head, pectoralis major, and posterior deltoid—were recorded from two separate groups of subjects ($n$ = 8 and 4, respectively). These supplementary behavioral data were obtained using a mock MRI. EMGs were rectified and band-pass filtered (20–200 Hz), and the average throughout the task was subtracted. A subject's EMGs from FCR, ECR, FCU, and ECU during the first set of the five [torques 1 and 2 (t1 and t2), cocontractions 1 and 2 (c1 and c2), and rest (r)] conditions are displayed in Fig. 2*A*.

*Task.* The subjects performed in five conditions: r, t1, c1, t2, and c2. Throughout the experiment, they received visual feedback of the applied torque and total muscle activation in the form of two bars (Fig. 1*B*). While the torque sensor reading was used as the visual feedback of torque, the visual feedback of total muscle activation was calcu-

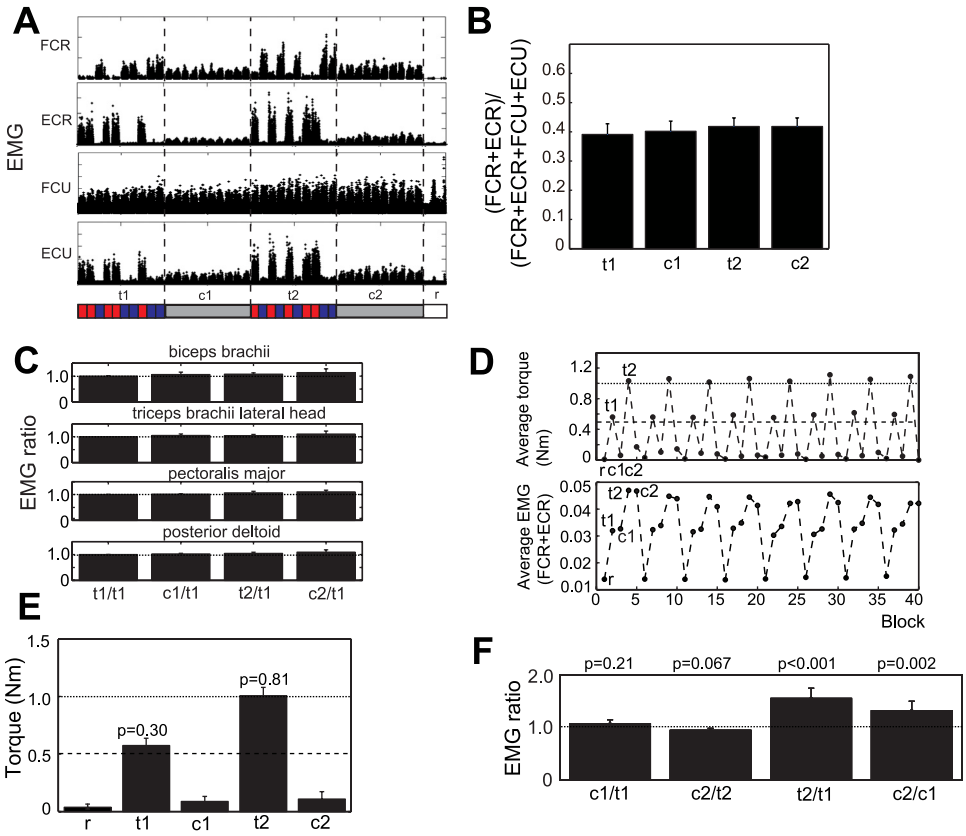


Fig. 2. Behavioral data and analysis. *A*: raw EMG data from a subject's wrist muscles—FCR, ECR, flexor carpi ulnaris (FCU), and extensor carpi ulnaris (ECU)—during the r, t1, c1, t2, and c2 conditions. The color marker below the condition indicates trial types (blue: flexion; red: extension; and gray: cocontraction). *B*: the EMG ratio (FCR + ECR)/(FCR + ECR + FCU + ECU) throughout the task was plotted for each condition. *C*: EMG data from upper-arm (biceps, triceps) and shoulder (pectoralis major and posterior deltoid) muscles plotted after normalizing with the activity during the t1 condition. These muscles did not show any significant chnage in activity across conditions. *D*: torque and integrated EMG of a typical subject show stable values over the task. Horizontal lines represent targets (0.5 Nm for t1 and 1.0 Nm for t2). Each point represents an average over 10 trials in 1 condition. *E*: mean torque and SD calculated across subjects show that torque was very small in the rest and cocontraction conditions. *F*: the ratios of EMG amplitude. c1 to t1 and c2 to t2 were not different from 1.0, and ratio t2 to t1 and c2 to c1 was significantly larger than 1.0.

lated as the summation of the rectified and smoothed EMG activity (see also section *EMG* above) from the antagonist wrist muscles ECR and FCR.

In each trial of the two torque conditions, subjects had to quickly increase their wrist torque to the target level and hold it during a 3-s target display period, after which, they could relax for 1 s (Fig. 1*B*) before a new target was presented. A series of 10 trials was performed in each condition block, in which the torque target was presented pseudorandomly to the left (i.e., flexion) or right (i.e., extension) directions (Fig. 1, *A* and *B*), and the numbers of the left and right trials were balanced (i.e., five). The target values of 0.5 Nm and 1.0 Nm were used in the t1 and t2 conditions, respectively.

In the cocontraction conditions, the subjects were required to increase their muscle activation to the target level by cocontracting the wrist flexor and extensor without applying any torque (i.e., keeping the torque bar at zero, Fig. 1*B*). The cocontraction target in each condition block was calculated by averaging the summation of the flexor and extensor muscle EMG signals recorded during the preceding torque condition block. Thus we balanced total EMG level between torque and cocontraction conditions. Similar to the torque conditions, the cocontraction target was also presented 10 times, randomly to the left or to the right, with five trials altogether in each direction. The change of the target location did not have a functional significance in this condition but ensured that the visual display resembled that of the torque conditions.

Note that the relative proximity of the target presentations in the torque condition and the slow blood oxygen level-dependent (BOLD) response ensure that brain activity, corresponding to both the flexor and extensor muscles (as detected by the fMRI), is active through the torque condition, although only the flexors or extensors were predominantly contracted at any one time. Therefore, the BOLD activity related to the total muscle activation, and the visual stimuli were equalized between the torque and cocontraction conditions, such that we could reasonably compare the neural activity in these conditions to identify the neural substrates for torque and cocontraction control.

The condition blocks (of r, t1, c1, t2, and c2) lasted for [30 s (rest) + 4 (conditions) × 10 (trials) × 4 s =] 190 s and were repeated eight times for a total experiment time of 1,520 s for each subject (Fig. 1*C*). All subjects had a practice session before the fMRI experiment to familiarize themselves with the paradigm and visual feedback and to avoid any learning-related effects during the scanning (see also RESULTS).

*fMRI.* A 1.5-T MRI scanner (Shimadzu-Marconi ECLIPSE 1.5T Power Drive 250) was used to obtain BOLD contrast functional images, which when weighted with the apparent transverse relaxation time, were obtained with a gradient echo echoplanar imaging (EPI) sequence. Data were collected from the whole brain. For each subject, 768 scans of BOLD images [repetition time 5.0 s, echo time 49 ms, flip angle 80°, field of view (FOV) 192 mm, resolution 3 × 3 × 5 mm, gap 1 mm, 64 × 64 in-plane voxels (in-plane FOV 224 $mm^2$)] were acquired. In addition to these experimental trials, each session contained six preliminary dummy scans to allow for T1 (short TR and short TE) equilibration effects. A custom-made bite bar was used in all experiments to reduce head movement, which resulted in head motion amplitude below 1 mm and 1° for all subjects. With these acquisition parameters, the parietal cortex was on the edge of the scope for several subjects; thus activity in the parietal cortex was excluded from subsequent fMRI analysis. However, data on the whole cerebellum, SMA, and PMd used for the analysis were available fully for all subjects.

*fMRI analysis.* EPI time series were preprocessed using a standard procedure in Statistical Parametric Mapping (SPM2) (Friston et al. 1995). The first six dummy volumes were discarded, and the remaining volumes were realigned to the first volume and unwarped. EPI and structural images were spatially normalized to the Montreal Neurological Institute (MNI) template embedded in SPM2. The normalized images were resliced into 2 × 2 × 2-mm voxels using the T2 (long TR and long TE) template of SPM and smoothed using an 8-mm full-width, half-maximum Gaussian kernel. The preprocessed data

were analyzed using random effect models (i.e., one-sample *t*-test) in SPM2 (Friston et al. 1995).

If neural activity specific to reciprocal activation were present, we hypothesize that it would increase with the torque amplitude in the torque conditions (Fig. 1*D*) and take similar low values in both the rest and cocontraction conditions. In contrast, neural activity specific to cocontraction control is expected to change with the amplitude of cocontraction in cocontraction conditions, with the rest and torque conditions taking similar low values (Fig. 1*D*).

The absolute value of torque averaged over each torque condition was used to create a parameterized block regressor for reciprocal activation conditions, while the r, c1, and c2 conditions were set to zero (Fig. 1*D*). Similarly, the average of two EMGs over each cocontraction condition was used to create a parametric block regressor for cocontraction conditions, while r, t1, and t2 were set to zero (Fig. 1*D*). These regressors were simultaneously fed to SPM with six dimensional movement parameters to isolate the neural correlates of reciprocal activation and cocontraction.

A parametric approach of fMRI data analysis (Haruno and Kawato 2006; Haruno et al. 2004) was preferred for identifying torque or cocontraction control-specific voxels over the conventional subtraction between torque and cocontraction conditions, since it also considers the amplitude of torque or cocontraction in the correlation analysis.

## RESULTS

*Behavioral data.* Figure 2*A* shows the raw EMGs of a typical subject recorded in a mock MRI. EMGs of FCR, ECR, FCU, and ECU are displayed for one set of conditions. We can see that both flexors and extensors were more active in t2 and c2 than in t1 and c1. Furthermore, flexors and extensors increased activity only in either flexion or extension trials, respectively, but coactivated in cocontraction conditions. These observations indicate that the subjects accurately maintained activity of each muscle with negligible cocontraction in torque conditions. It is also noteworthy that FCR and ECR were not the only muscles involved in the task, but flexors (FCR and FCU) and extensors (ECR and ECU) exhibited synchronized activity in torque and cocontraction conditions, although a level of noise was seen in the FCU. Note that the muscle activation ratio (FCR + ECR)/(FCR + ECR + FCU + ECU) was indistinguishable across the two torque and two cocontraction conditions (Fig. 2*B*; $P > 0.45$, *t*-test). This indicates that the sum of the activations in these four task-related muscles (Hoffman and Strick 1999) was linearly related to the sum of FCR and ECR in our isometric setup. Therefore, the EMG signals of the two, FCR and ECR, could be used to isolate brain activity, corresponding to all of the muscles in the fMRI analysis, which is based on linear regression.

In general, while the muscles of the upper-arm can accompany contractions of the wrist muscles (Humphrey and Reed 1983), for low-strength isometric contractions, as in the current study, the muscle moment arms remain approximately constant (Winter 1990). Therefore, the upper-arm and shoulder muscles were predicted to be similarly activated between the torque and cocontraction conditions. This was confirmed by the similar muscle activity across various conditions of the experiment (Fig. 2*C*).

Figure 2*D* shows the average torque and average total EMG (FCR + ECR) over blocks of a typical subject performing a series of condition sequences in the fMRI scanner: r, t1, c1, t2, and c2. The averaged torque (Fig. 2*E*) and cocontraction (Fig. 2*F*) over all of the subjects exhibited four important characteristics. First, the torque in the rest condition was not different from zero ($P > 0.76$). Second, the torques in t1 and t2 conditions were not different from the target values of 0.5 Nm ($P = 0.30$) and 1.0 Nm ($P = 0.81$), respectively, and did not change over time (Fig. 2*D*). Third, the torque in the two cocontraction conditions was also almost zero. Fourth, EMG amplitude was similar in t1 and c1 conditions (i.e., their ratio was not significantly different from 1.0; $P = 0.21$) and also in t2 and c2 ($P = 0.067$), but it was substantially different between t1 and t2 and c1 and c2 (Fig. 2*F*; $P < 0.002$).

*Neural correlates of total muscle activity.* We asked the subjects to exert torque in the two opposite directions (flexion and extension). Therefore, even though the different conditions in the experiment required torque or cocontraction control, the same set of muscles was used as actuators in different combinations to achieve both. To investigate the neural correlates of these commonly activated muscles, a block-design correlation analysis of the fMRI data was carried out with a regressor parameterized by the total mean EMG in each block [Fig. 2*D*; $P < 0.001$, uncorrected; voxel cluster size >10 voxels included; SPM random effect model (Friston et al. 1995)].

Activity was observed in the left M1 (Fig. 3*A*). The average of the BOLD activity from the peak coordinates (−42, −18, 54) of all subjects (Fig. 3*B*) illustrates that this location in M1 was not activated at rest and was similarly active in t1 and c1 ($P > 0.45$, *t*-test), as well as in t2 and c2 ($P > 0.33$, *t*-test). Furthermore, the activity was very different between these two torque-cocontraction sets; i.e., the activity ratio during t2 and c2 was significantly different from the activity during t1 and c1 ($P < 0.001$): almost twice as large. In addition, at least 10 consecutive voxels around the peaks showed substantial similarity to the peak activity. This suggests that our setup was able to detect functionally correct motor areas.

*Brain regions selectively involved in reciprocal muscle control.* To analyze the fMRI activity specific to reciprocal activation, we conducted a linear regression of BOLD signal ($P < 0.001$, uncorrected; voxel cluster size >10; SPM2 random effect model) (Friston et al. 1995) with each subject's torque regressor (Fig. 1*D*). Activity-correlated torque was detected in the boundary between the posterior part of the left PMd (peak voxel) and left M1 (Fig. 4*A*) and in the anterior cerebellum (Fig. 4*C*). The MNI coordinates of the peak voxels were (−26, −8, 54) and (14, −46, −22), respectively.

Figure 4, *B* and *D*, summarizes the across-subject results, displaying the BOLD signal increase of the same peak voxels [(−26, −8, 54) and (14, −46, −22), respectively], averaged over trials and subjects. BOLD signals were significantly larger in t2 than in t1 ($P < 0.001$ for the PMd in Fig. 4*B*, and $P < 0.01$ for the cerebellum in Fig. 4*D*), and the values of rest and cocontraction conditions were much smaller than in t1 ($P < 0.05$ for Fig. 4*B*, *t*-test). Additionally, Fig. 4, *B* and *D*, indicates that the BOLD difference between t1 and t2 was more prominent in the PMd than in the cerebellum. This may reflect functional differences between these two regions. When we made the statistical threshold lower ($P < 0.005$, uncorrected; voxel cluster size >10), correlation in the PMd and cerebellum became bilateral, and the SMA also appeared (Table 1).

Finally, Fig. 5 contrasts M1 peak activity correlated with total EMG (Fig. 3*A*) and PMd peak activity correlated with torque with a stringent statistical threshold ($P < 0.0005$,

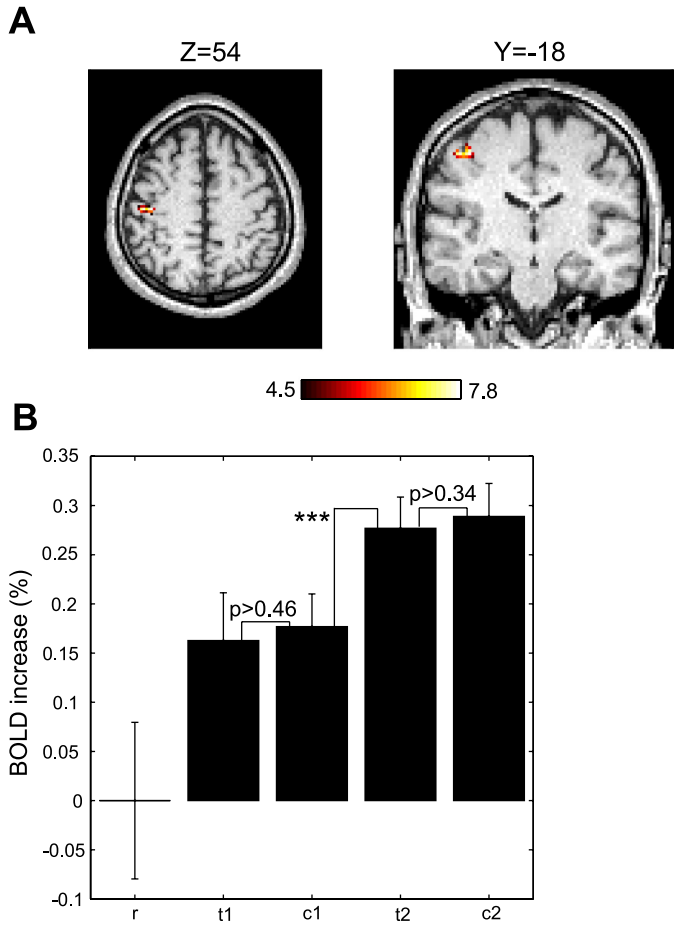


Fig. 3. Neural correlates of total muscle activity. To investigate the neural correlates of the muscles used in both torque and cocontraction conditions, a regression was performed with total EMG throughout the experiment. Functional MRI activity in the primary motor cortex (M1) was correlated with total muscle activity (second panel of Fig. 2*D*) during both torque and cocontraction conditions. *A*: significant activity over 12 subjects [$P < 0.001$, uncorrected, 1-sample *t*-test; Statistical Parametric Mapping (SPM2), cluster size >10] in the M1. The peak voxel of the Montreal Neurological Institute (MNI) coordinates was (−42, −18, 54). *B*: the voxel activity over 12 subjects at the same coordinates shows similar activity in t1 and c1 ($P > .46$) and t2 and c2 ($P > 0.34$), respectively. Throughout the subsequent figures, we indicate statistics as $*P < 0.05$, $**P < 0.01$, and $***P < 0.001$. The color bars represent *t*-values in the rest of figures. BOLD, blood oxygen level dependent.

uncorrected; voxel cluster size >10). The peak voxel with torque is located more anterior in the PMd, whereas the peak voxel with total EMG is located more posterior in the M1.

*Brain regions selectively involved in cocontraction control.* To detect the neural correlates of cocontraction control, a regressor focusing on cocontraction periods was built by using the mean EMG of the major extensor ECR and flexor FCR and by setting zero during the rest and reciprocal activation conditions (Fig. 1*D* and METHODS). BOLD activity that correlated with this cocontraction regressor ($P < 0.001$, uncorrected; voxel cluster size >10; SPM random effect model) was found on the left PMv (Fig. 6*A*), with the peak voxel at (−60, 6, 12) in the MNI coordinates. Correlation was also found in the left putamen and M1 but was less significant than that of the PMv (Table 1).

Figure 6*B* summarizes the across-subject results of the BOLD signal increase of the same peak voxel (−60, 6, 12) averaged over trials and subjects. BOLD signal was significantly ($P < 0.05$, *t*-test) larger in c2 than in c1, and the values in the torque conditions were significantly ($P < 0.01$ between c1 and t2, *t*-test) smaller than in the cocontraction conditions and not different between these two conditions ($P > 0.09$ between t1 and t2, *t*-test).

When the statistical threshold was lowered to $P < 0.005$, uncorrected; voxel cluster size >10, activity in the SMA became visible for both torque and cocontraction conditions, similar to M1 (Table 1). This activity was found to be posterior to the anterior commissure and confined in the SMA proper.

## DISCUSSION

This study examined the neural substrates for the voluntary control of reciprocal activation and the cocontraction of muscles using fMRI with a MRI-compatible manipulandum and real-time feedback of EMG. Activity in the caudo-PMd and the anterior cerebellum was found to be correlated with torque, and the PMv activity was modulated by the cocontraction level. These findings reveal the key role of the premotor cortices in the voluntary control of reciprocal activation and the cocontraction of muscles.

We also found that the M1 and SMA were involved in both tasks (Table 1), consistent with previous studies (Dai et al. 2001; Dettmers et al. 1995; Pope et al. 2005; Vaillancourt et al. 2003). In addition, activity in the cerebellum and putamen was differentially correlated with torque and cocontraction level, respectively. This dissociation of the subcortical areas was consistent with the reported inability to control cocontraction in dystonia patients, which is believed to be caused by deficits in the putamen.

The PMd has been reported to be involved in force generation (Dai et al. 2001; Dettmers et al. 1995; Pope et al. 2005; Vaillancourt et al. 2003) and the spatial representation of task goals (Halsband and Passingham 1985; Jackson and Husain 1996; Kurata and Hoffman 1994; Majdandzic et al. 2009; Pesaran et al. 2006). Our results agree with these previous findings. However, since we contrasted activity with the cocontraction condition, which specifies muscle activity but no direction, the PMd differences in our study might reflect some higher-level mapping between motor output and direction (Hoshi and Tanji 2007). However, this is improbable, because the activity in the PMd was correlated with the amplitude of torque, which would not be expected in higher-level mechanisms.

On the other hand, the PMv is known to be active, specifically during precision grip tasks (Davare et al. 2006), which are expected to require cocontraction control for precise interaction with external objects (Majdandzic et al. 2009). A fMRI study of reaching movements with a joystick (Seidler et al. 2004) reported that the PMv is one of the areas that showed a negative correlation to target size, whereas activity in the PMd increased with target size. This observation could be explained by the involvement of the PMv in control of impedance [which is directly related to cocontraction and known to be negatively correlated with target size in goal-directed reaching (Osu et al. 2004; Selen et al. 2006)].

One may expect that differences in neural activity between the torque and cocontraction conditions originated from differences in arm-muscle activation or tactile feedback in the two conditions. We confirmed that external arm muscles do not

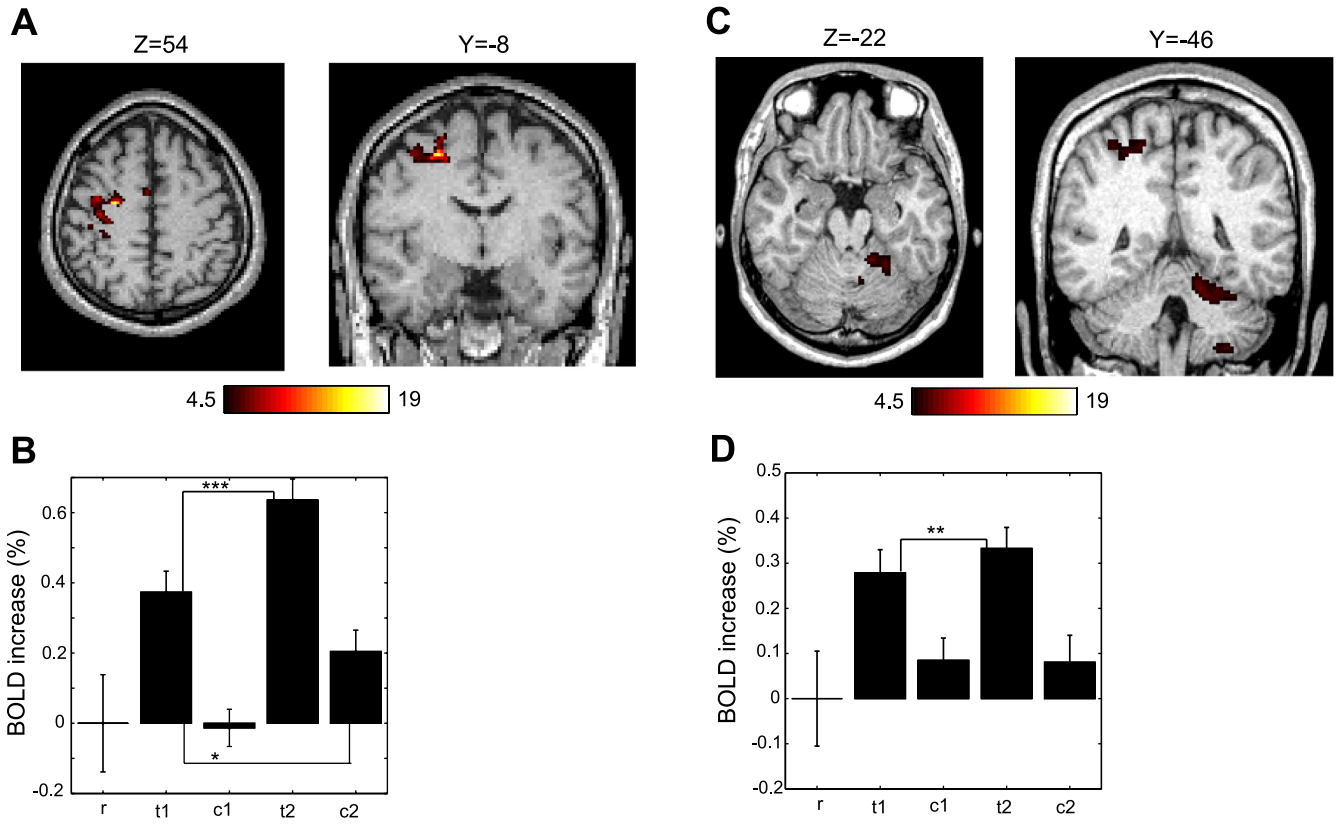


Fig. 4. Brain regions selectively involved in reciprocal muscle control. BOLD activity in the dorsal premotor cortex (PMd) was correlated with torque. *A*: significant activity over 12 subjects ($P < 0.001$, uncorrected, 1-sample *t*-test; SPM2; cluster size >10) is detected in the left PMd with peak activity in the voxel (−26, −8, 54 MNI coordinates). *B*: BOLD percentage increases in the same peak voxel, averaged in a block and then over all subjects, are significantly higher in the torque conditions than in the cocontraction conditions. This activity shows a remarkable correlation of the voxel activity with the torque regressor (first panel of Figs. 2*D* and 1*D*). *C*: right anterior cerebellum activity is also correlated with torque ($P < 0.001$, uncorrected, 1-sample *t*-test; SPM2; cluster size >10). *D*: the peak BOLD activity in the anterior cerebellum peak (14, −46, −22 MNI coordinates) averaged over the 12 subjects is correlated with wrist torque.

contribute to the results (Fig. 2*C*) but are unable to confirm the same for inner arm muscles, which are difficult to measure in our setup. To check for possible tactile differences, we conducted a control experiment of passive wrist movement with the same fMRI-compatible device (Fig. 1*A*), where the brain received tactile feedback information but did not generate any motor commands. Under these conditions, brain activation was observed in the somatosensory area, the M1, and the anterior cerebellum but not in the premotor cortex. Conversely, we did not find any activity in the somatosensory area during regression with torque and during comparison of the torque and cocontraction conditions. These results suggest that tactile feedback was not the cause of the observed results.

Table 1. *Summary of activity correlated with torque and cocontraction*

| Structure | Torque | Cocontraction |
|---|---|---|
| L PMd | (−26, −8, 54) | |
| R PMd | (28, −4, 48) ($P < 0.005$) | |
| L PMv | | (−60, 6, 12) |
| R PMv | | |
| L M1 | (−38, −16, 62) | (−24, −20, 62) |
| R M1 | | |
| L CB | (−28, −48, −32) ($P < 0.005$) | |
| R CB | (14, −46, −22) | |
| SMA | (−4, 0, 52) ($P < 0.005$) | (−2, −4, 62) ($P < 0.005$) |
| L Putamen | | (−22, −2, −4) |

The statistical threshold adopted was $P < 0.001$, uncorrected for multiple comparison, and cluster size >10, otherwise explicitly stated as $P < 0.005$. L, left; R, right; PMd, dorsal premotor cortex; PMv, ventral premotor cortex; M1, primary motor cortex; CB, cerebellum; and SMA, supplementary motor area.

What makes control of cocontraction distinct from reciprocal activation? Cocontraction in real life is usually accompanied by force control. This is evident, for example, in the precision grip of an egg, where a precise cocontraction level is used to enable precision control of the grip force. We tried to recreate a similar environment in our experiment, where in the cocontraction conditions, the subjects also had to maintain the torque bar at zero. It could be argued that cocontraction control is inherently more difficult than force control, and the reason behind the PMv activation is related to this. However, it is important to note that this "difficulty" is due to differences in the control requirements that are inherent to the cocontraction task and not just due to differences in the involved muscles or in their activation levels (which were equalized between the conditions). In this respect, the findings of this paper clarify that the antagonist muscles require a different or additional brain region when they are controlled simultaneously.

The fact that activity in the PMd better reflects a difference in torque amplitude (Fig. 4*B*) than the PMv in coactivation (Fig. 6*B*) might suggest a hierarchical structure (Evarts 1981) existing behind muscle control: the PMv coactivates antagonist muscle groups by regulating a set of the M1 neuron pools, each

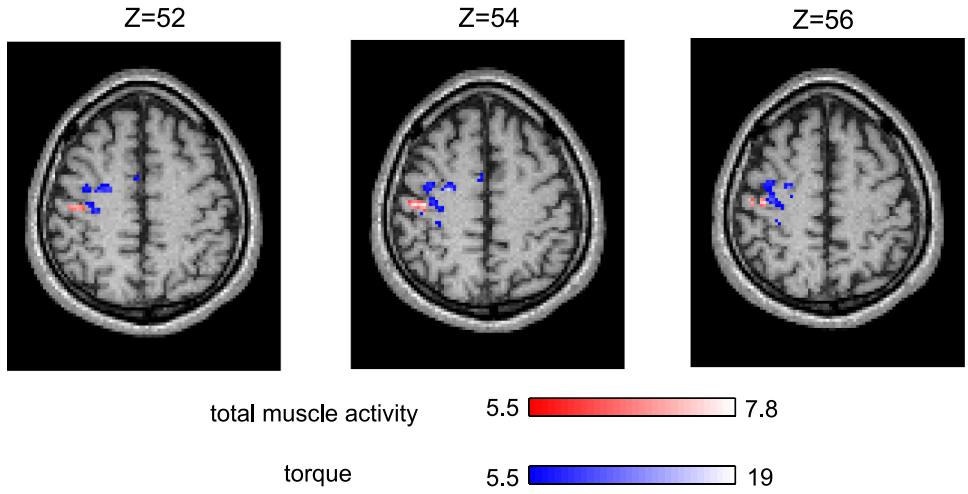


Fig. 5. Contrast between the PMd and M1. The peak voxels with surrounding activity for both torque (Fig. 4*A*) and total muscle activity (Fig. 3*A*) are displayed on the same map with a stringent statistical threshold ($P < 0.0005$ uncorrected; cluster size >10). This figure shows that activity correlated with torque is more anteriorly located in the PMd than activity correlated with total muscle activity.

of which controls a few similarly acting muscles (Umilta et al. 2007), whereas in reciprocal activation, the PMd may only control the smaller M1 neuronal pools, which project to a few target muscles (Fetz and Cheney 1980; Jackson et al. 2003; Rathelot and Strick 2006). Alternatively, the PMd and PMv may also regulate different subpopulations of M1 neurons in the current task, as reported previously for wrist-arm movements (Strick and Preston 1979). However, the presence of numerous intermingled neural circuits in M1 (Fetz and Cheney 1980; Graziano 2006; Jackson et al. 2003; Rathelot and Strick 2006) and limited spatial resolution of fMRI make it difficult to precisely identify the functional representation in M1 at present.

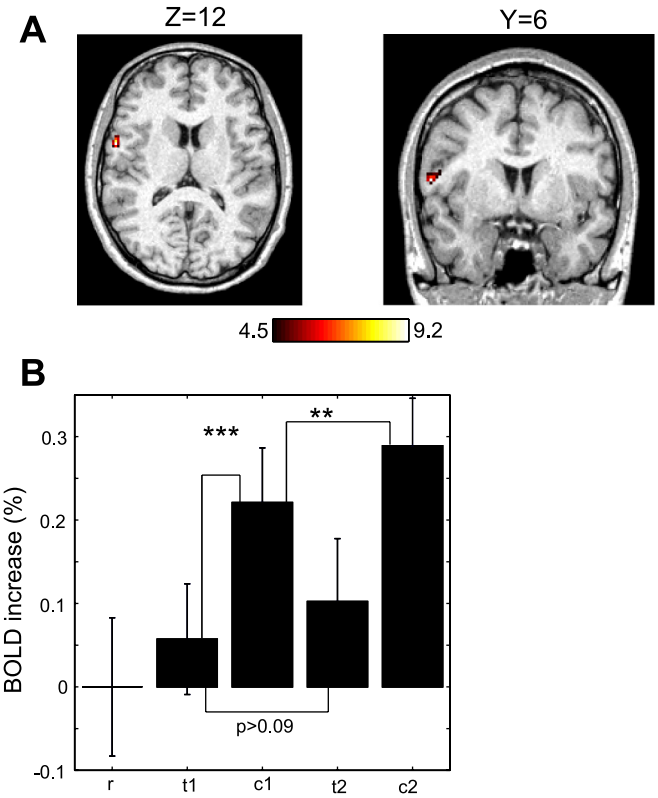


Fig. 6. Brain regions selectively involved in cocontraction control. Brain activity correlated with the EMG level during cocontraction. *A*: statistically significant correlation with EMG over 12 subjects ($P < 0.001$, uncorrected, 1-sample *t*-test; SPM2; cluster size >10) shows activity in the left ventral premotor cortex with peak activity in the voxel (−60, 6, 12 MNI coordinates). *B*: the average of peak activity across subjects shows significantly larger activity in the cocontraction than in the torque conditions. The mean activity during the cocontraction conditions increases with the cocontraction level ($P < 0.01$).

In summary, the results of our experiment indicate that the differential centers of the premotor cortex are related to the control of reciprocal activation and cocontraction. This suggests that distinct processes may be used by the CNS to control force and impedance, consistent with the specific inability to control cocontraction observed in dystonia patients (Berardelli et al. 1998). These findings provide a cohesive explanation for previous reports of premotor activation, as was detailed above. Precise information about the regulation of reciprocal activation and cocontraction performed by the premotor cortex could be gained through electrical recording in nonhuman primates and by performing the experiment analyzed in this paper with human patients.

## ACKNOWLEDGMENTS

We thank S. Tada, I. Fujimoto, Y. Shimada, and Y. Furukawa for technical assistance and K. Savin for helpful comments about the manuscript.

## GRANTS

Support for this research was provided by the Strategic Research Program for Brain Sciences (SRPBS) and a contract with the National Institute of Information and Communications Technology, entitled "Multimodal integration for brain imaging measurements" to M. Kawato. Support for M. Haruno was provided by PRESTO/JST and KAKENHI (22300139). Support for E. Burdet was provided by the EU FP7 Human Behavioral Modeling for Enhancing Learning by Optimizing Human-Robot Interaction (HUMOUR) project.

## DISCLOSURES

No conflicts of interest, financial or otherwise, are declared by the author(s).

## AUTHOR CONTRIBUTIONS

Author contributions: M.H. conception and design of research; M.H. and G.G. performed experiments; M.H. and G.G. analyzed data; M.H., G.G., E.B., and M.K. interpreted results of experiments; M.H. prepared figures; M.H. drafted manuscript; M.H., G.G., E.B., and M.K. edited and revised manuscript; M.H., G.G., E.B., and M.K. approved final version of manuscript.

## REFERENCES


**Berardelli A, Rothwell JC, Hallett M, Thompson PD, Manfredi M, Marsden CD.** The pathophysiology of primary dystonia. *Brain* 121: 1195–1212, 1998.

**Bizzi E, Accornero N, Chapple W, Hogan N.** Posture control and trajectory formation during arm movement. *J Neurosci* 4: 2738–2744, 1984.

**Burdet E, Osu R, Franklin DW, Milner TE, Kawato M.** The central nervous system stabilizes unstable dynamics by learning optimal impedance. *Nature* 414: 446–449, 2001.

**Cheney PD, Fetz EE.** Functional classes of primate corticomotoneuronal cells and their relation to active force. *J Neurophysiol* 44: 773–791, 1980.

**Dai TH, Liu JZ, Sahgal V, Brown RW, Yue GH.** Relationship between muscle output and functional MRI-measured brain activation. *Exp Brain Res* 140: 290–300, 2001.

**Damm L, McIntyre J.** Physiological basis of limb-impedance modulation during free and constrained movements. *J Neurophysiol* 100: 2577–2588, 2008.

**Davare M, Andres M, Cosnard G, Thonnard JL, Olivier E.** Dissociating the role of ventral and dorsal premotor cortex in precision grasping. *J Neurosci* 26: 2260–2268, 2006.

**Dettmers CF, Fink GR, Lemon RN, Stephan KM, Passingham RE, Silberseig D, Holmes A, Ridding MC, Brooks DJ, and Frackowiak RS.** Relation between cerebral activity and force in the motor areas of human brain. *J Neurophysiol* 74: 802–815, 1995.

**Evarts EV.** Relation of pyramidal tract activity to force exerted during voluntary movement. *J Neurophysiol* 24: 83–86, 1968.

**Evarts EV.** Roles of motor cortex in voluntary movements in primates. In: *Handbook of Physiology, The Nervous System II*. Bethesda, MD: American Physiological Society, 1981, p. 1083–1112.

**Feldman AG.** Functional tuning of the nervous system with control of movement or maintenance of a steady posture. III. Mechanographic analysis of execution by man of the simplest motor tasks. *Biophysics* 11: 766–775, 1966.

**Fetz EE, Cheney PD.** Postspike facilitation of forelimb muscle activity by primate corticomotoneuronal cells. *J Neurophysiol* 44: 751–771, 1980.

**Franklin DW, Burdet E, Tee KP, Osu R, Chew CM, Milner TE, Kawato M.** CNS learns stable, accurate, and efficient movements using a simple algorithm. *J Neurosci* 28: 11165–11173, 2008.

**Friston KJ, Holmes AP, Worsley K, Poline JB, Frith C, Frackowiak RSJ.** Statistical parametric maps in functional brain imaging: a general linear approach. *Hum Brain Mapp* 2: 189–210, 1995.

**Ganesh G, Franklin DW, Gassert R, Imamizu H, Kawato M.** Accurate real-time feedback of surface EMG during fMRI. *J Neurophysiol* 97: 912–920, 2007.

**Gassert R, Moser R, Burdet E, Bleuler H.** MRI/fMRI-compatible robotic system with force feedback for interaction with human motion. *IEEE/ASME Trans Mechatron* 11: 216–224, 2006.

**Graziano M.** The organization of behavioral repertoire in motor cortex. *Annu Rev Neurosci* 29: 105–134, 2006.

**Halsband U, Passingham RE.** Premotor cortex and the conditions for movement in monkeys (*Macaca fascicularis*). *Behav Brain Res* 18: 269–277, 1985.

**Haruno M, Kawato M.** Different neural correlates of reward expectation and reward expectation error in putamen and caudate nucleus during stimulus-action-reward association learning. *J Neurophysiol* 95: 948–959, 2006.

**Haruno M, Kuroda T, Doya K, Toyama K, Kimura M, Samejima K, Imamizu H, Kawato M.** A neural correlate of reward-based behavioral learning in caudate nucleus: a functional magnetic resonance imaging study of a stochastic decision task. *J Neurosci* 24:1660–1665, 2004.

**Haruno M, Wolpert DM.** Optimal control of redundant muscles in step-tracking wrist movements. *J Neurophysiol* 94: 4244–4255, 2005.

**Hoffman DS, Strick PL.** Step-tracking movements of the wrist. IV. Muscle activity associated with movements in different directions. *J Neurophysiol* 81: 319–333, 1999.

**Hoshi E, Tanji J.** Distinctions between dorsal and ventral premotor areas: anatomical connectivity and functional properties. *Curr Opin Neurobiol* 17: 234–242, 2007.

**Humphrey DR, Reed DJ.** Separate cortical systems for control of joint movement and joint stiffness: reciprocal activation and co-contraction of antagonist muscles. In: *Motor Control Mechanisms in Health and Disease*, edited by Desmedt JE. New York: Raven, 1983, p. 347–342.

**Jackson A, Gee VJ, Baker SN, Lemon RN.** Synchrony between neurons with similar muscle fields in monkey motor cortex. *Neuron* 38: 115–125, 2003.

**Jackson SR, Husain M.** Visuomotor functions of the lateral premotor cortex. *Curr Opin Neurobiol* 6: 788–795, 1996.

**Kakei S, Hoffman D, Strick PL.** Muscle and movement representations in the primary motor cortex. *Science* 24: 2136–2139, 1999.

**Kurata K, Hoffman DS.** Differential effects of muscimol microinjection into dorsal and ventral aspects of the premotor cortex of monkeys. *J Neurophysiol 71*: 1151–1164, 1994.

**Lacquaniti F, Maioli C.** The role of preparation in tuning anticipatory and reflex responses during catching. *J Neurosci* 9: 134–148, 1989.

**Levin MF, Feldman AG, Milner TE, Lamarre Y.** Reciprocal and coactivation commands for fast wrist movements. *Exp Brain Res* 89: 669–677, 1992.

**Majdandzic J, Bekkering H, van Schie HT, Toni I.** Movement-specific repetition suppression in ventral and dorsal premotor cortex during action observation. *Cereb Cortex* 19: 2736–2745, 2009.

**Ostry DJ, Feldman AG.** A critical evaluation of the force control hypothesis in motor control. *Exp Brain Res* 153: 275–288, 2003.

**Osu R, Kamimura N, Iwasaki H, Nakano E, Harris CM, Wada Y, Kawato M.** Optimal impedance control for task achievement in the presence of signal-dependent noise. *J Neurophysiol* 92: 1199–1215, 2004.

**Perreault EJ, Kirsch RF, Crago PE.** Effects of voluntary force generation on the elastic components of endpoint stiffness. *Exp Brain Res* 141: 312–323, 2001.

**Pesaran B, Nelson MJ, Andersen RA.** Dorsal premotor neurons encode the relative position of the hand, eye, and goal during reach planning. *Neuron* 51: 125–134, 2006.

**Pope P, Wing AM, Praamstra P, Miall RC.** Force related activations in rhythmic sequence production. *Neuroimage* 27: 909–918, 2005.

**Rathelot JA, Strick PL.** Muscle representation in the macaque motor cortex: an anatomical perspective. *Proc Natl Acad Sci USA* 23: 8257–8262, 2006.

**Seidler RD, Noll DC, Thiers G.** Feedforward and feedback processes in motor control. *Neuroimage* 22: 1775–1783, 2004.

**Selen LP, van Dieën JH, & Beek PJ.** Impedance modulation and feedback corrections in tracking targets of variable size and frequency. *J Neurophysiol* 96: 2750–2759, 2006.

**Strick PL, Preston JB.** Multiple representation in the motor cortex; a new concept of input-output organization for the forearm representation. In: *Integration in the Nervous System*, edited by Asanuma H. and Wilson VJ. Tokyo: Igakushoin, 1979, p. 205–221.

**Umilta MA, Brochier T, Spinks RL, Lemon RN.** Simultaneous recording of macaque premotor and primary motor cortex neuronal populations reveals different functional contributions to visuomotor grasp. *J Neurophysiol* 98: 488–501, 2007.

**Vaillancourt DE, Thulborn KR, Corcos DM.** Neural basis for the processes that underlie visually guided and internally guided force control in humans. *J Neurophysiol* 90: 3330–3340, 2003.

**Winter DA.** *Biomechanics and Motor Control of Human Movement*. New York: John Wiley & Sons, 1990.